

Nuclear shadowing in polarized deep inelastic scattering on ${}^6\text{LiD}$ at small x and its effect on the extraction of the deuteron spin structure function $g_1^d(x, Q^2)$

V. Guzey

Special Research Centre for the Subatomic Structure of Matter (CSSM), Adelaide University, Adelaide 5005, Australia

(Received 16 May 2001; published 27 August 2001)

We consider the effect of nuclear shadowing in polarized deep inelastic scattering (DIS) on ${}^6\text{LiD}$ at small Bjorken x and its relevance for the extraction of the deuteron spin structure function $g_1^d(x, Q^2)$. Using models, which describe nuclear shadowing in unpolarized DIS, we demonstrate that the nuclear shadowing correction to $g_1^d(x, Q^2)$ is significant.

DOI: 10.1103/PhysRevC.64.045201

PACS number(s): 24.85.+p, 21.45.+v, 13.60.Hb

I. INTRODUCTION

Recent interest in the spin structure of the proton, neutron, and deuteron and advances in experimental techniques have led to a number of experiments concerned with deep inelastic scattering (DIS) of polarized leptons on various polarized targets. Among these are the E143 experiment at SLAC [1] and the SMC Collaboration at CERN [2], which used polarized hydrogen and deuterium, the E154 experiment at SLAC [3] and the HERMES Collaboration at DESY [4], which used polarized ${}^3\text{He}$, and the HERMES experiment [5], which used polarized hydrogen [5].

A new material, deuterized lithium ${}^6\text{LiD}$, has recently emerged as a source of polarized deuterium in the E155/E155x experiments at SLAC. In comparison with the previously used target materials, ${}^6\text{LiD}$ shows a better dilution factor (polarizability) and radiation resistance (durability) [6]. The deuteron spin structure function $g_1^d(x, Q^2)$ was studied with the use of the polarized ${}^6\text{LiD}$ target by the SLAC E155 experiment for the first time [7].

In order to extract the spin structure functions of the proton, neutron, and deuteron from the polarized DIS data on nuclear targets one needs to account for nuclear effects. These effects can be divided into incoherent and coherent contributions.

The incoherent nuclear effects result from the scattering of the incoming lepton on each individual nucleon, nucleon resonance, or virtual meson in the nucleus. The incoherent nuclear effects are present at all Bjorken x . Spin depolarization, the presence of non-nucleonic degrees of freedom, Fermi motion, binding, and off-shell effects are examples of incoherent nuclear effects.

In the target rest frame, coherent nuclear effects arise from the interaction of the incoming lepton with two or more nucleons of the target. The coherent nuclear effects are typically concentrated at low values of Bjorken x . Nuclear shadowing at $10^{-4} \leq x \leq 0.05$ and subsequent antishadowing at $0.05 \leq x \leq 0.2$ are examples of coherent effects. It is important to stress that the transition between the shadowing and antishadowing regions is not well understood. Thus, the Bjorken x , where the transition occurs, is known only approximately. For example, the NMC unpolarized DIS data on nuclei [8] suggests that, depending on the nuclear target, the

transition takes place¹ between $x = 0.02$ and $x = 0.07$. Consequently, one can reliably estimate the effect of nuclear shadowing only at $x \leq 0.02$.

In case of polarized DIS on nuclear targets, the major nuclear effect is spin depolarization. This effect manifests itself as a decrease of the effective polarization of the nucleons due to the presence of higher partial waves in bound-state nuclear wave functions [9]. The effective polarization P of a nucleon is introduced as the probability that the nucleon carries spin of the fully polarized nuclear target. P can be reliably calculated by the standard methods of nuclear physics.

As an example, one can consider the proton and neutron effective polarizations in the deuteron, defined as $P_n = P_p = 1 - 1.5 \omega_D$, where ω_D is the probability of the D wave in the deuteron ground-state wave function. One finds that $P_n = P_p = 0.913$, using the Paris nucleon-nucleon potential [10], and $P_n = P_p = 0.936$, using the Bonn nucleon-nucleon potential [11].

As another example, one can consider the effective polarizations of the neutron and protons in ${}^3\text{He}$. Calculations of the ${}^3\text{He}$ bound-state wave function with various nucleon-nucleon potentials and three-nucleon forces yield significant probabilities of higher partial waves. This results in the following effective polarizations: $P_n = 0.86 \pm 0.02$ for the neutron and $P_p = -0.028 \pm 0.004$ for each proton [12].

In case of the target of ${}^6\text{LiD}$, polarized deuterium originates from deuterons D as well as from ${}^6\text{Li}$ since the latter can be visualized, to a first approximation, as an α particle plus a polarized deuteron. Treating ${}^6\text{Li}$ as a cluster $\alpha + p + n$, the Faddeev equation for the three-body system can be used to calculate the properties of the ground-state wave function of ${}^6\text{Li}$. The calculations of Ref. [13] indicate that the effective polarizations of the proton and neutron in polarized ${}^6\text{Li}$ are $P_n = P_p = 0.866 \pm 0.012$ [6]. In addition to this effect, an isotopic analysis of the ${}^6\text{LiD}$ target revealed that 4.6% of lithium is ${}^7\text{Li}$ and that 2.4% of deuterium is hydrogen [6]. And, finally, the effective polarization of ${}^6\text{Li}$ was measured to be 97% of the polarization of the free deuterons in ${}^6\text{LiD}$ [7]. Thus, assuming that ${}^6\text{LiD}$ is fully polar-

¹According to the NMC data [8], nuclear shadowing disappears at $x = 0.0175$ for ${}^6\text{Li}$ and at $x = 0.07$ for ${}^{40}\text{Ca}$.

ized with $P_{6\text{LiD}}=1$, the effective polarization of deuterium in ${}^6\text{LiD}$ is

$$P_d = \frac{1}{2} \left(0.976 + \frac{0.97 \times 0.954 \times 0.866}{1 - 1.5 \omega_D} \right) = 0.916 - 0.927 \pm 0.013, \quad (1)$$

where the first (second) value is for the Bonn (Paris) nucleon-nucleon potential.

Also, in order to extract the precise shape of the proton, neutron, or deuteron spin structure function $g_1(x, Q^2)$ from the DIS data on polarized nuclear targets, one must account for the Fermi motion, binding, and off-shell effects. However, calculations for deuterium [14] and for ${}^3\text{He}$ [15] indicate that these effects are negligible at $x \leq 0.7$. Thus, with good accuracy one can neglect them while extracting $g_1^d(x, Q^2)$ from the ${}^6\text{LiD}$ data at $x \leq 0.7$.

The importance of the deuteron spin depolarization in ${}^6\text{LiD}$ [see Eq. (1)] is well established and has been taken into account in analyzing the data of the E155 experiment [7]. However, since some of the data covers the interval of small Bjorken x , $0.014 \leq x \leq 0.2$, corrections should be made for nuclear shadowing and antishadowing. As explained above, this region of x corresponds to the transition between the regimes of nuclear shadowing and antishadowing, which is known very poorly at the moment. Thus, one cannot estimate the effect of nuclear shadowing at $x \geq 0.02$ until a theory of antishadowing exists. Consequently, in this work, we estimate the effect of nuclear shadowing in polarized DIS on ${}^6\text{LiD}$ and its influence on the extraction of $g_1^d(x, Q^2)$ at very small Bjorken x only, $10^{-4} \leq x \leq 0.02$. Our analysis is applicable only to the lowest E155 point $\langle x \rangle = 0.015$.

II. NUCLEAR SHADOWING AND ANTISHADOWING EFFECTS

As explained in the Introduction, the polarization of ${}^6\text{LiD}$ is formed by the effective polarizations of deuterons, ${}^6\text{Li}$, protons, and ${}^7\text{Li}$. Neglecting the Fermi motion, binding, and off-shell effects, the spin structure function of ${}^6\text{LiD}$ $g_1^{6\text{LiD}}(x, Q^2)$ can be written as

$$g_1^{6\text{LiD}}(x, Q^2) = 0.976 g_1^d(x, Q^2) + 0.97 \times 0.954 g_1^{6\text{Li}}(x, Q^2) + 0.024 g_1^p(x, Q^2) + 0.046 \times 0.97 g_1^{7\text{Li}}(x, Q^2). \quad (2)$$

Equation (2) assumes that the admixtures of hydrogen and ${}^7\text{Li}$ to ${}^6\text{LiD}$ are 100 and 97% polarized, respectively.

Equation (2) neglects the nuclear shadowing and antishadowing corrections. Their importance in unpolarized and polarized DIS at small Bjorken x is well understood (for a recent review see Ref. [16]). In the laboratory reference frame, nuclear shadowing arises from the interaction of the incoming lepton with two and more nucleons of the target. These multiple interactions decrease total inclusive cross

sections in unpolarized DIS as well as spin asymmetries in polarized DIS. The latter fact results in a decrease of $g_1^{6\text{LiD}}(x, Q^2)$

$$g_1^{6\text{LiD}}(x, Q^2) = 0.976 g_1^d(x, Q^2) + 0.925 g_1^{6\text{Li}}(x, Q^2) + 0.024 g_1^p(x, Q^2) + 0.045 g_1^{7\text{Li}}(x, Q^2) - 0.976 \delta g_1^d(x, Q^2) - 0.925 \delta g_1^{6\text{Li}}(x, Q^2) - 0.045 \delta g_1^{7\text{Li}}(x, Q^2), \quad (3)$$

where $\delta g_1^d(x, Q^2)$, $\delta g_1^{6\text{Li}}(x, Q^2)$, and $\delta g_1^{7\text{Li}}(x, Q^2)$ denote the shadowing corrections for the corresponding spin structure functions. Thus, Eq. (3) describes the ${}^6\text{LiD}$ spin structure function $g_1^{6\text{LiD}}(x, Q^2)$ and the corrections associated with nuclear shadowing² at small Bjorken x , $10^{-4} - 10^{-3} \leq x \leq 0.02 - 0.05$.

The amount of nuclear shadowing in Eq. (3) is expected to be significant due to two reasons. Firstly, shadowing corrections to the spin dependent structure functions $g_1(x, Q^2)$ are about twice as large as those to the spin-averaged structure functions $F_2(x, Q^2)$ [17–19]. Secondly, shadowing corrections are larger for heavier nuclei. Since almost half of the polarized deuterons in ${}^6\text{LiD}$ originate from ${}^6\text{Li}$, where the nuclear shadowing correction is significant, the shadowing corrections to $g_1^{6\text{Li}}(x, Q^2)$ are larger than those to $g_1^d(x, Q^2)$.

The shadowing corrections for the deuteron spin structure function were calculated in Ref. [19]. It was found that the ratio $\delta g_1^d(x, Q^2) / [g_1^p(x, Q^2) + g_1^n(x, Q^2)]$ is, for example, 0.058 at $x = 10^{-3}$ and 0.048 at $x = 10^{-2}$.

Within the framework developed in Refs. [17,18], one can estimate the nuclear shadowing corrections to $g_1^{6\text{Li}}(x, Q^2)$ and $g_1^{7\text{Li}}(x, Q^2)$ using the Gribov-Glauber multiple scattering formalism along with simple ground-state wave functions of ${}^6\text{Li}$ and ${}^7\text{Li}$. The details of this calculation are presented in the Appendix.

The amount of nuclear shadowing depends on the effective cross section of the incoming photon-nucleon interaction σ_{eff} , see Eq. (A4). We have considered two representative examples of σ_{eff} existing in the literature. These are the σ_{eff} , which can be inferred from the two-phase model of nuclear shadowing of Ref. [21], and the σ_{eff} from the leading-twist diffraction-based approach to nuclear shadowing of Ref. [22]. The main difference between the two models is different parametrizations of the Pomeron contribution. Figure 1 represents σ_{eff} of Ref. [21] as a solid line and σ_{eff} of Ref. [22] as a dashed line.

At very low Bjorken x , calculations with both σ_{eff} predict a similar amount of nuclear shadowing. Namely, at $x = 10^{-4} - 10^{-3}$ and $Q^2 = 4 \text{ GeV}^2$, the ratio

²The upper limit for nuclear shadowing $x \approx 0.05$ is usually estimated as the Bjorken x , when the coherence length $l_c = 1/(2m_N x)$ is equal to 1.7 fm, the average internucleon distance in nuclei.

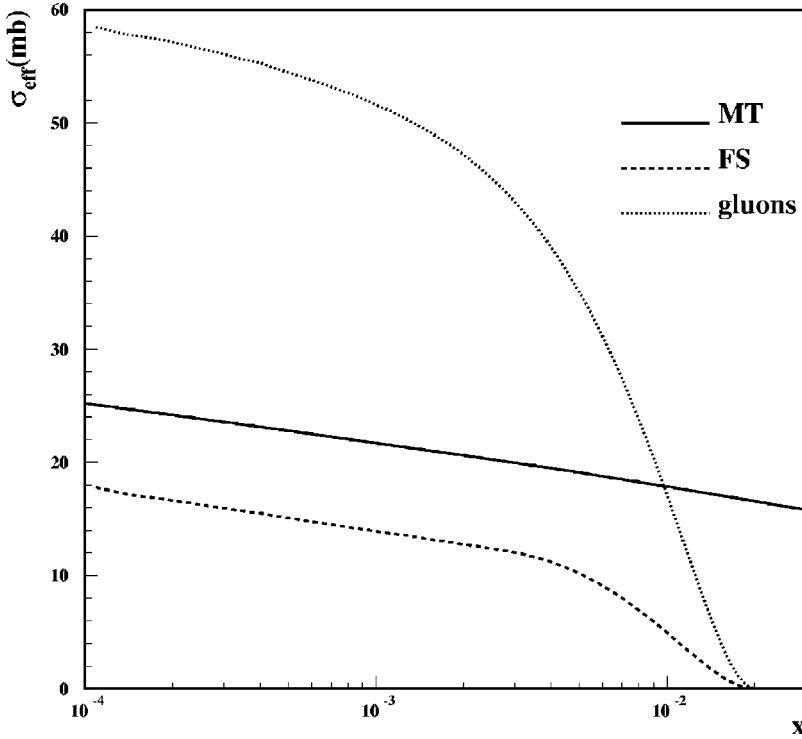


FIG. 1. Two scenarios for σ_{eff} as a function of x at $Q_0^2=4 \text{ GeV}^2$. The solid line represents σ_{eff} inferred from the two-phase model of Ref. [21]. The dashed line is from the leading-twist diffraction-based picture of nuclear shadowing of Ref. [22]. The dotted line represents σ_{eff} of Ref. [22] for the gluon-induced nuclear shadowing.

$\delta g_1^{6\text{Li}}(x, Q^2)/[g_1^p(x, Q^2) + g_1^n(x, Q^2)]$ equals 0.17–0.15 (0.12–0.10) for σ_{eff} given by the solid (dashed) curve in Fig. 1. However, at larger x , the deviation between the predictions made with the two scenarios for σ_{eff} becomes larger. While, for example, at $Q^2=4 \text{ GeV}^2$ and $x=10^{-2}$, $\delta g_1^{6\text{Li}}(x, Q^2)/[g_1^p(x, Q^2) + g_1^n(x, Q^2)]=0.12$ for the calculation with the σ_{eff} of Ref. [21], $\delta g_1^{6\text{Li}}(x, Q^2)/[g_1^p(x, Q^2) + g_1^n(x, Q^2)]=0.03$ for the calculation with the σ_{eff} of Ref. [22].

Note also that at even larger x , $x \approx 0.02\text{--}0.05$, the calculations of nuclear shadowing bear a significant theoretical uncertainty. At those values of x , the coherent length of the incident photon becomes comparable to the average internucleon distance in nuclei and, as a consequence, nuclear shadowing rapidly decreases and gives up its place to antishadowing. The position and shape of this transition is unknown. Thus, we estimate the effect of nuclear shadowing only at $10^{-4} \leq x \leq 0.02$.

The shadowing correction to the ${}^7\text{Li}$ spin structure function, given by Eq. (A5), is not only sizable but also does not vanish when $g_1^d(x, Q^2)$ vanishes. Thus, at those Bjorken x , where $g_1^d(x, Q^2)$ is small and, hence, $\delta g_1^d(x, Q^2)$ and $\delta g_1^{6\text{Li}}(x, Q^2)$ are small, the term proportional to $\delta g_1^{7\text{Li}}(x, Q^2)$ in Eq. (3) gives the dominant contribution to the shadowing correction to $g_1^{6\text{LiD}}(x, Q^2)$ regardless the fact that ${}^7\text{Li}$ is only a 4.6% admixture to ${}^6\text{LiD}$. At other values of x , $\delta g_1^{7\text{Li}}(x, Q^2)$ in Eq. (3) can be safely neglected.

Nuclear shadowing at $10^{-4} \leq x \leq 0.05$ is followed by some antishadowing at $0.05 \leq x \leq 0.2$, which enhances $g_1^{6\text{LiD}}(x, Q^2)$ above the impulse approximation prediction of Eq. (2). In unpolarized DIS, the presence of this enhancement for the nuclear structure function $F_{2A}(x, Q^2)$ and the

gluon and valence quark parton densities in nuclei has firm experimental evidence (see Ref. [16] for a review). However, since the understanding of the dynamics of nuclear antishadowing is lacking, it can only be treated in a model-dependent way. For example, in Ref. [23], the contribution of antishadowing was modeled using the baryon number and momentum sum rules for the nucleus.

In polarized DIS, antishadowing is not constrained by the baryon number and momentum sum rules. However, in the particular case of polarized DIS on mirror nuclei, one can use the generalization of the Bjorken sum rule [17]. Using this approach, the antishadowing contribution to the nonsinglet nuclear spin structure function $g_1^{\text{NS}}(x, Q^2)$ of ${}^3\text{He}$ [17,18] and ${}^7\text{Li}$ [18] was modeled. The contribution was found to be of the order of 14–40% for the $A=3$ system and of the order of 20–55% for the $A=7$ system. The spread of the presented values is an indication of the uncertainty of where the transition between the shadowing and antishadowing regions takes place.

Although the generalization of the Bjorken sum rule for ${}^6\text{LiD}$ does not exist because ${}^6\text{LiD}$ is an isoscalar, there is no reason for the absence of the antishadowing correction in DIS on polarized ${}^6\text{LiD}$. While nuclear antishadowing is expected to modify the extraction of $g_1^d(x, Q^2)$ from the ${}^6\text{LiD}$ data at $0.02\text{--}0.05 \leq x \leq 0.2$, we do not estimate this effect and simply confine our predictions to the nuclear shadowing range of x , $10^{-4} \leq x \leq 0.02$.

In this work, the shadowing correction to $g_1^{6\text{LiD}}(x, Q^2)$ is calculated using Eq. (3) at a fixed low scale $Q^2=Q_0^2=4 \text{ GeV}^2$. In order to find the modification of $g_1^{6\text{LiD}}(x, Q^2)$ due to the nuclear effects at larger Q^2 , $Q^2 > Q_0^2$, the QCD evolution with the input, described by Eq. (3), should be

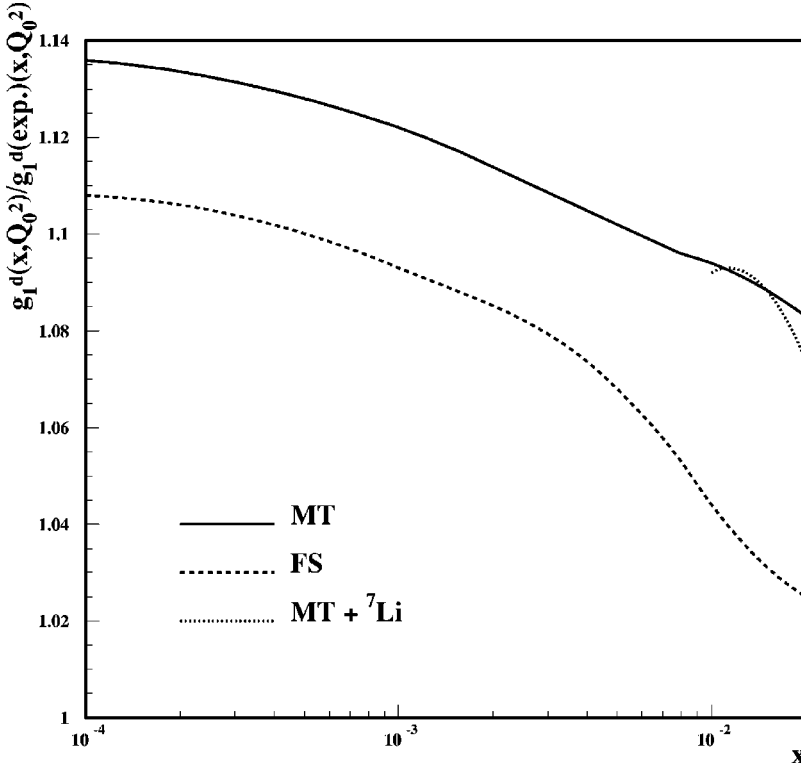


FIG. 2. The ratio $g_1^d(x, Q_0^2)/g_{1 \text{ exp}}^d(x, Q_0^2)$ of Eq. (4) as a function of x at $Q_0^2 = 4 \text{ GeV}^2$. The solid line is the result of the calculation with σ_{eff} of Ref. [21] without the $\delta g_1^{7\text{Li}}(x, Q^2)$ term in Eq. (4). $g_1^d(x, Q^2)/g_{1 \text{ exp}}^d(x, Q^2)$ with the $\delta g_1^{7\text{Li}}(x, Q^2)$ term included, where applicable, is given by the dotted line. The calculation with σ_{eff} of Ref. [22] is presented as a dashed line.

used. Based on the experience from the QCD evolution of unpolarized parton densities, it is expected that nuclear shadowing at small Bjorken x and high Q^2 will decrease because of the contribution of the polarized gluons originating from the unshadowed, high x , region at the initial evolution scale Q_0^2 .

Now we are in position to give an estimate of the importance of the shadowing correction in Eq. (3) on the extraction of the deuteron spin structure function $g_1^d(x, Q^2)$. Let us denote by $g_{1 \text{ exp}}^d(x, Q^2)$ the deuteron spin structure function in the impulse approximation, i.e., $g_{1 \text{ exp}}^d(x, Q^2)$ is obtained from Eq. (2) where the coherent effects at small Bjorken x are neglected. The ratio of the theoretical prediction for $g_1^d(x, Q^2)$, given by Eq. (3), when the effect of shadowing is present, and $g_{1 \text{ exp}}^d(x, Q^2)$ is presented as

$$\frac{g_1^d(x, Q^2)}{g_{1 \text{ exp}}^d(x, Q^2)} = 1 + \frac{1}{2P_d g_{1 \text{ exp}}^d(x, Q^2)} [0.976 \delta g_1^d(x, Q^2) + 0.925 \delta g_1^{6\text{Li}}(x, Q^2) + 0.045 \delta g_1^{7\text{Li}}(x, Q^2)], \quad (4)$$

where P_d is given by Eq. (1). Note that the ratio $g_1^d(x, Q^2)/g_{1 \text{ exp}}^d(x, Q^2)$ is equal to unity if the effect of nuclear shadowing is neglected.

It is important to stress that the quantity, which is measured in polarized DIS, is the spin asymmetry A_{\parallel} , where $A_{\parallel} \approx g_{1 \text{ exp}}^d(x, Q^2)/F_1(x, Q^2)$. Then, in polarized DIS, one obtains $g_{1 \text{ exp}}^d(x, Q^2)$ by multiplying A_{\parallel} by the spin-averaged structure function $F_1(x, Q^2)$, which is also experimentally measured and, therefore, contains all nuclear effects. The lat-

ter fact is true for the E155 experiment data analysis [20], regardless the fact that it is not apparent from the E155 publication [7]. Thus, Eq. (4) indeed describes the shadowing correction to the experimentally measured $g_{1 \text{ exp}}^d(x, Q^2)$.

Using the results of Ref. [19] for $\delta g_1^d(x, Q^2)$ and of the Appendix for $\delta g_1^{6\text{Li}}(x, Q^2)$ and $\delta g_1^{7\text{Li}}(x, Q^2)$, the ratio $g_1^d(x, Q^2)/g_{1 \text{ exp}}^d(x, Q^2)$ of Eq. (4) is presented as a function of x at $Q_0^2 = 4 \text{ GeV}^2$ in Fig. 2.

The solid line is a result of the calculation without the $\delta g_1^{7\text{Li}}(x, Q^2)$ term. The ratio $g_1^d(x, Q^2)/g_{1 \text{ exp}}^d(x, Q^2)$ with the $\delta g_1^{7\text{Li}}(x, Q^2)$ term included is presented as the dotted line. These two curves are obtained using σ_{eff} of the two-phase model of Ref. [21]. The shadowing correction to $g_1^{7\text{Li}}(x, Q^2)$ was calculated by Eq. (A5). Since the deuteron spin structure function parametrization of Ref. [7] covers the region of $x \geq 0.01$, the contribution of the $\delta g_1^{7\text{Li}}(x, Q^2)$ term starts at $x = 0.01$ in Fig. 2.

The calculation with the leading-twist σ_{eff} of Ref. [22] is presented by the dashed line in Fig. 2. In this case, the term proportional to $\delta g_1^{7\text{Li}}(x, Q^2)$ does not contribute to the net shadowing correction to $g_1^{6\text{Li}}(x, Q^2)$ because σ_{eff} is negligibly small at $x \geq 0.01$, where $g_1^d(x, Q^2)$ is parametrized and sizable.

The results of the calculations with the Paris and Bonn nucleon-nucleon potentials are virtually the same. In Fig. 2, the Paris nucleon-nucleon potential for ω_D is used.

Figure 2 illustrates that, at small Bjorken x , $10^{-4} \leq x \leq 10^{-3}$, the shadowing correction is a slow function of x , i.e., shadowing is saturated, and it works to increase $g_{1 \text{ exp}}^d(x, Q^2)$ by 13.5–12% for the calculation with σ_{eff} of

Ref. [21] and by 11.5–10 % for the calculation with σ_{eff} of Ref. [22]. At $x \geq 10^{-3}$ the shadowing correction begins to decrease more rapidly as a function of x . For the lowest data point of the E155 experiment $\langle x \rangle = 0.015$, we predict that $g_1^d(x, Q^2)/g_{1\text{exp}}^d(x, Q^2)$ could still be as large as 1.09 for the calculation with σ_{eff} of Ref. [21]. Thus, we conclude that nuclear shadowing does modify the extraction of the deuteron spin structure function $g_1^d(x, Q^2)$ from $g_1^{6\text{LiD}}(x, Q^2)$ at $x = 10^{-4} \leq x \leq 0.02$.

Note also that, since the E155 data [7] indicates that $|g_1^d(x, Q^2)|$ is nonzero and quite significant at small Bjorken x , the shadowing correction $\delta g_1^d(x, Q^2)$ is important for the extraction of the neutron spin structure function $g_1^n(x, Q^2)$ from $g_1^d(x, Q^2)$.

While the present day data on $g_1^d(x, Q^2)$ is not accurate enough to demonstrate the importance of nuclear shadowing, in the future, when high precision data at even lower x becomes available, the importance of nuclear effects typical for low Bjorken x can be unambiguously established. Moreover, with high precision polarized DIS data one can study the role played by polarized gluons. Since, in unpolarized DIS, nuclear shadowing in the gluon channel is expected to be 3 times larger than in the sea quark channel (see Fig. 1 for the the corresponding σ_{eff}), the shadowing correction to the polarized nuclear gluon parton density could be 3 times larger than that to the structure function $g_1(x, Q^2)$ [18].

III. CONCLUSIONS

The recent SLAC E155 experiment used deuterized lithium (${}^6\text{LiD}$) as a source of polarized deuterons in order to study the deuteron spin structure function $g_1^d(x, Q^2)$ at $0.014 \leq x \leq 0.9$. Since some of the data covers the region of small Bjorken x , $0.014 \leq x \leq 0.05$, where nuclear shadowing and antishadowing play an important role, necessary corrections should be made.

In this work we considered nuclear shadowing in polarized DIS on the ${}^6\text{LiD}$ target and its effect on the spin structure function $g_1^{6\text{LiD}}(x, Q^2)$ at small Bjorken x , $10^{-4} \leq x \leq 0.02$. The previous analysis of polarized DIS on deuterium, ${}^3\text{He}$ and ${}^7\text{Li}$ suggests that the effect of nuclear shadowing in the nuclear spin dependent structure functions $g_1^A(x, Q^2)$ is enhanced by a factor of 2 as compared to the spin-averaged structure functions $F_{2A}(x, Q^2)$.

The magnitude of the nuclear shadowing effect is represented using the ratio $g_1^d(x, Q^2)/g_{1\text{exp}}^d(x, Q^2)$ [see Eq. (4)]. While, in the absence of the shadowing corrections, the ratio $g_1^d(x, Q^2)/g_{1\text{exp}}^d(x, Q^2)$ equals unity, nuclear shadowing at $x = 10^{-4} - 10^{-3}$ increases the ratio above unity by 13.5–12 % for the calculation with the σ_{eff} extracted from Ref. [21] and by 11.5–10 % for the calculation with σ_{eff} of Ref. [22]. For the lowest data point of the E155 experiment $\langle x \rangle = 0.015$, the shadowing correction to the ratio $g_1^d(x, Q^2)/g_{1\text{exp}}^d(x, Q^2)$ could be as large as 9%. Therefore, nuclear shadowing does modify the extraction of $g_1^d(x, Q^2)$ from $g_1^{6\text{LiD}}(x, Q^2)$ in the range of $10^{-4} \leq x \leq 0.02$ and, consequently, affects the extraction of $g_1^n(x, Q^2)$ from $g_1^d(x, Q^2)$.

Further theoretical effort is required to understand the dynamical mechanism of antishadowing, which was not discussed in this work.

Finally, we would like to stress that the phenomenon of nuclear shadowing in polarized DIS on nuclear targets is a genuine low x nuclear effect, which should be treated on the equal footing with any other nuclear effect, such as, for instance, spin depolarization.

ACKNOWLEDGMENTS

I would like to thank Mark Strikman and Anthony W. Thomas for helpful comments and discussions, Kazuo Tsushima for pointing out and discussing Refs. [26,27], and George Smirnov for commenting on an early draft of this paper. This work was partially supported by the Australian Research Council.

APPENDIX: DERIVATION OF THE NUCLEAR SHADOWING CORRECTION FOR POLARIZED DIS ON ${}^6\text{Li}$ AND ${}^7\text{Li}$

In this appendix, we outline key steps in the derivation of the shadowing contribution in polarized DIS on the ${}^6\text{Li}$ and ${}^7\text{Li}$ targets. In our analysis, we will closely follow the approach presented in Refs. [17,18].

In the laboratory reference frame, the incoming polarized photon with the high energy ν , momentum q , four-momentum Q^2 and small Bjorken x interacts with the hadronic target by means of its coherent quark-gluon fluctuations $|h_i\rangle$

$$\sigma_{\gamma^*A}(\nu, Q^2) = \sum_i |\langle \gamma^* | h_i \rangle|^2 \sigma_{h_iA}(\nu, Q^2), \quad (\text{A1})$$

where σ_{γ^*A} and σ_{h_iA} are the photon and $|h_i\rangle$ nucleus cross sections, respectively; $|\langle \gamma^* | h_i \rangle|^2$ is the probability to find the configuration $|h_i\rangle$ in the photon wave function.

Following Refs. [17,18], we have replaced the sum in Eq. (A1) by a single effective fluctuation $|h_{\text{eff}}\rangle$ with $M_{h_{\text{eff}}}^2 \approx Q^2$ and the $|h_{\text{eff}}\rangle$ -nucleon scattering cross section σ_{eff} . We have also made a hypothesis that σ_{eff} in polarized DIS is the same as in the unpolarized DIS. We considered two following models for σ_{eff} .

Using the connection between the leading contribution to nuclear shadowing, proportional to σ_{eff} , and diffractive scattering on the proton, $\gamma^* + p \rightarrow X + p'$, the leading-twist model for σ_{eff} was derived in Ref. [22]. The dashed line in Fig. 2, denoted as ‘‘FS,’’ represents the corresponding σ_{eff} as a function of x at $Q_0 = 2$ GeV.

Note also that a similar value of σ_{eff} at $x = 10^{-3}$ and Q^2 equal a few GeV^2 can be extracted from the analysis of nuclear shadowing in unpolarized DIS on nuclei with $A \geq 12$.

The two-phase model of nuclear shadowing of Ref. [21] was successfully applied in unpolarized DIS on light and heavy nuclei in order to describe the experimental data on the ratio F_{2A}/F_{2D} . The corresponding σ_{eff} contains both the leading-twist (Pomeron and triple Pomeron) and subleading-

twist (vector mesons) contributions. It is presented as a solid line in Fig. 2 and is denoted as “MT.”

Thus, we used the models for σ_{eff} of Refs. [22,21] as estimates of the lower and upper limits for the amount of nuclear shadowing in polarized DIS on ${}^6\text{Li}$ and ${}^7\text{Li}$. Within the discussed one-state approximation, the photon-nucleus cross section is proportional to the $|h_{\text{eff}}\rangle$ -nucleus cross section

$$\sigma_{\gamma^*A}(\nu, Q^2) \propto \sigma_{h_{\text{eff}}A}(\nu, Q^2). \quad (\text{A2})$$

The latter can be calculated using the Gribov-Glauber multiple scattering formalism [24,25], generalized to include the non-zero longitudinal momentum transferred to the target $q_{\parallel} \approx 2m_N x$, which leads to an x dependence of nuclear shadowing. The Gribov-Glauber scattering formalism requires the knowledge of the nuclear ground-state wave function and the elementary $|h_{\text{eff}}\rangle$ -nucleon scattering amplitude.

Simple forms for the ground-state wave functions of polarized ${}^6\text{Li}$ and ${}^7\text{Li}$ are assumed. In ${}^6\text{Li}$, one proton and one neutron are polarized with the effective polarization $P = 0.866$. The effective polarization of the valence nucleons (predominantly the proton) of the ${}^7\text{Li}$ ground-state wave function is given by the nuclear shell-model expression [18]. In addition, the distribution of the nucleons in the configuration space, given by the square of the corresponding wave function, is taken as a simple Gaussian shape

$$|\Psi_{{}^6\text{Li}, {}^7\text{Li}}|^2 \propto \exp\left(-\frac{3}{2} \frac{r^2}{\langle r^2 \rangle}\right), \quad (\text{A3})$$

where $\langle r^2 \rangle$ is the average electromagnetic radius of the nucleus. $\langle r^2 \rangle^{1/2} = 2.56 \pm 0.10$ fm for ${}^6\text{Li}$ [26] and $\langle r^2 \rangle^{1/2} = 2.41 \pm 0.10$ fm for ${}^7\text{Li}$ [27]. Note that nucleon-nucleon correlations in the nuclear wave functions (A3) are neglected. This is a good approximation for the low Bjorken x , $10^{-4} \leq x \leq 0.02$, considered in this work. The $|h_{\text{eff}}\rangle$ -nucleon scattering amplitude is chosen to be purely imaginary with $B = 6 \text{ GeV}^{-2}$ being the slope of the $|h_{\text{eff}}\rangle$ -nucleon cross section.

Keeping the double and triple scattering contributions, the nuclear shadowing correction to the spin structure function $g_1^{\text{Li}}(x, Q^2)$ can be presented as

$$\begin{aligned} \delta g_1^{\text{Li}}(x, Q^2) = & \left(5 \frac{\sigma_{\text{eff}}}{4\pi(\langle r^2 \rangle/3 + B)} e^{-q_{\parallel}^2 \langle r^2 \rangle/3} \right. \\ & \left. - 10 \frac{(\sigma_{\text{eff}})^2}{48\pi^2(\langle r^2 \rangle/3 + B)^2} g(x) \right) P_n [g_1^p(x, Q^2) \\ & + g_1^n(x, Q^2)], \end{aligned} \quad (\text{A4})$$

where $g(x)$ is a weak function of x , normalized as $g(0) = 1$.

The shadowing correction, described by Eq. (A4), depends on the value of σ_{eff} . Using the “MT” (“FS”) scenario for σ_{eff} , one finds that the ratio $\delta g_1^{\text{Li}}(x, Q^2)/[g_1^p(x, Q^2) + g_1^n(x, Q^2)]$ equals 0.17 (0.12) at $x = 10^{-4}$, 0.15 (0.10) at $x = 10^{-3}$, and 0.12 (0.3) at $x = 0.01$.

Using Eq. (7) of Ref. [18] along with the numerical values for the corresponding constants, the nuclear shadowing correction to the spin dependent structure function of ${}^7\text{Li}$, $\delta g_1^{\text{Li}}(x, Q^2)$, can be presented in the following form:

$$\begin{aligned} \delta g_1^{\text{Li}}(x, Q^2) = & \sigma_{\text{eff}} \{ 7.62 \times 10^{-3} g_1^p(x, Q^2) + 1.51 \\ & \times 10^{-3} [g_1^p(x, Q^2) + g_1^n(x, Q^2)] \} e^{-176x^2} \\ & - (\sigma_{\text{eff}})^2 \{ 4.08 \times 10^{-5} g_1^p(x, Q^2) + 8.65 \\ & \times 10^{-6} [g_1^p(x, Q^2) + g_1^n(x, Q^2)] \} \tilde{g}(x), \end{aligned} \quad (\text{A5})$$

where $\tilde{g}(x)$ is a slow function of x , normalized as $\tilde{g}(0) = 1$. Equation (A5) includes the double and triple scattering contributions to $\delta g_1^{\text{Li}}(x, Q^2)$. Higher multiple scattering order terms are negligibly small.

Unlike $\delta g_1^d(x, Q^2)$ and $\delta g_1^{\text{Li}}(x, Q^2)$, $\delta g_1^{\text{Li}}(x, Q^2)$ is not proportional to $g_1^p(x, Q^2) + g_1^n(x, Q^2)$. Thus, at those Bjorken x , where $g_1^p(x, Q^2) + g_1^n(x, Q^2)$ and, hence, $\delta g_1^d(x, Q^2)$ and $\delta g_1^{\text{Li}}(x, Q^2)$ vanish, in spite of ${}^7\text{Li}$ being a small admixture to ${}^6\text{Li}$ D, $\delta g_1^{\text{Li}}(x, Q^2)$ becomes significant (see the dotted line in Fig. 1).

-
- [1] E143 Collaboration, K. Abe *et al.*, Phys. Rev. D **58**, 112003 (1998).
[2] SMC Collaboration, B. Adeva *et al.*, Phys. Rev. D **58**, 112001 (1998).
[3] E154 Collaboration, K. Abe *et al.*, Phys. Lett. B **405**, 180 (1997); K. Abe *et al.*, Phys. Rev. Lett. **79**, 26 (1997).
[4] HERMES Collaboration, K. Ackerstaff *et al.*, Phys. Lett. B **404**, 383 (1997).
[5] HERMES Collaboration, A. Airapetian *et al.*, Phys. Lett. B **442**, 484 (1998).
[6] S. Bultmann *et al.*, Report No. SLAC-PUB-7904, 1998.
[7] E155 Collaboration, P.L. Anthony *et al.*, Phys. Lett. B **463**, 339 (1999).
[8] NMC Collaboration, P. Amaudruz *et al.*, Phys. Lett. B **441**, 3 (1995); M. Arneodo *et al.*, *ibid.* **441**, 12 (1995).
[9] B. Blankleider and R.M. Woloshyn, Phys. Rev. C **29**, 538 (1984).
[10] M. Lacombe, B. Loiseau, J.M. Richard, and R.V. Mau, Phys. Rev. C **21**, 861 (1980).
[11] R. Machleidt, K. Holinde, and C. Elster, Phys. Rep. **149**, 1 (1987).
[12] J.L. Friar, B.F. Gibson, G.L. Payne, A.M. Bernstein, and T.E. Chupp, Phys. Rev. C **42**, 2310 (1990).
[13] N.W. Schellingerhout *et al.*, Phys. Rev. C **48**, 2714 (1993); **52**, 439 (1995).
[14] L. Frankfurt and M. Strikman, Nucl. Phys. **A405**, 557 (1983);

- W. Melnitchouk, G. Piller, and A.W. Thomas, Phys. Lett. B **346**, 165 (1995); S.A. Kulagin *et al.*, Phys. Rev. C **52**, 932 (1995).
- [15] C. Ciofi degli Atti, S. Scopetta, E. Pace, and G. Salme, Phys. Rev. C **48**, R968 (1993).
- [16] G. Piller and W. Weise, Phys. Rep. **330**, 1 (2000).
- [17] L. Frankfurt, V. Guzey, and M. Strikman, Phys. Lett. B **381**, 379 (1996).
- [18] V. Guzey and M. Strikman, Phys. Rev. C **61**, 014002 (2000).
- [19] J. Edelman, G. Piller, and W. Weise, Z. Phys. A **357**, 129 (1997); Phys. Rev. C **57**, 3392 (1998).
- [20] M. Strikman (private communication with S. Rock).
- [21] W. Melnitchouk and A.W. Thomas, Phys. Lett. B **317**, 437 (1993); Phys. Rev. C **52**, 3373 (1995); J. Kwiecinski and B. Badelek, Phys. Lett. B **208**, 508 (1988).
- [22] L. Frankfurt and M. Strikman, Eur. Phys. J. A **5**, 293 (1999).
- [23] L.L. Frankfurt and M.I. Strikman, Phys. Rep. **160**, 235 (1988); L.L. Frankfurt, M.I. Strikman, and S. Liuti, Phys. Rev. Lett. **65**, 1725 (1990).
- [24] R.J. Glauber, Phys. Rev. **100**, 242 (1955).
- [25] V.N. Gribov, Sov. J. Nucl. Phys. **9**, 369 (1969); Sov. Phys. JETP **29**, 483 (1969); **30**, 709 (1970).
- [26] I. Tanihata *et al.*, Phys. Rev. Lett. **55**, 2676 (1985).
- [27] H. De Vries, C.W. De Jager, and C. De Vries, At. Data Nucl. Data Tables **36**, 495 (1987).